Materials Research Proceedings **26** (2023) 29-34 https://doi.org/10.21741/9781644902431-5

# Fracturing process in an anisotropic layered geomaterial: theoretical and computational predictions

Martina Rinaldi[1,a], Marco Trullo[1,b] , Francesco Tornabene[1,c] and Rossana Dimitri[1,d*]

[1]Department of Innovation Engineering, Università del Salento, 73100, Lecce, Italy

[a]martina.rinaldi@unisalento.it, [b]marco.trullo@unisalento.it, [c]francesco.tornabene@unisalento.it, [d*]rossana.dimitri@unisalento.it

**Keywords:** Anisotropic Geomaterials, Fracture Mechanics, XFEM

**Abstract.** The present work investigates the fracturing behavior of an anisotropic layered geomaterial, known as Opalinus Clay (OPA). The formation of this rock is mainly related to a sedimentation process, where bedding planes correspond to planes of isotropy. OPA is here studied because of its good properties, primarily, the low permeability and high adsorption capability, which make it a perfect candidate for the storage of radioactive waste. The characterization of this rock takes place experimentally in the Mont Terri Rock Laboratory, in the northern Switzerland, with an increased attention to theoretical and computational predictions. In this context, this work aims at simulating the nonlinear crack behavior of OPA by using the eXtended Finite Element Method (XFEM) and damage mechanics. The study is applied on a Semi-Circular specimen under a Bending load (SCB), whose fracturing response is investigated in terms of peak load and direction of the cracking propagation for different notch dimensions and geometries.

## Introduction

An underground capability in which radioactive waste can be permanently stored, is called deep geological repository. Based on studies conducted in the Mont Terri Rock laboratory, OPA has been identified as a capable material of hosting high-level radioactive Waste. In order to define the feasibility of such repository, the rock must be characterized in its fracturing behavior, which is highly affected by its mechanical anisotropy [1-3]. In the last years, Barbi et al. [4] applied on OPA the design parameters defined experimentally by Bock [5], i.e. deformability, strength, permeability and hydro-mechanically-coupled parameters, and studied the orientation-dependence of fracture mechanics parameters for SCB tests. Following the studies [4,6] , and based on the pioneering work by Bock [5], we here evaluate comparatively, the SCB behavior as provided by an advanced computational XFEM and damage concepts. This falls within a wider numerical investigation, as provided in Ref. [7], focusing on the force-CMOD response, together with the specimen toughness and kinematic behavior.

Due to the efficient kinematic approximation at the interfacial level, and the proper introduction of discontinuous enrichment functions, the XFEM is capable to avoid very fine mesh refinements ahead of the crack tip, to follow a crack propagation [8-12]. The main XFEM basics are, thus, applied to model the crack propagation in transversely-isotropic geomaterials, accounting for a standard SCB test, which is explored in its fracturing response for different notch shapes and sizes, in terms of global response, maximum strength, toughness and cracking propagation. After a brief description of the XFEM theoretical basics, we discuss about the numerical investigation and results, focusing on the overall sensitivity of the response.

## Theoretical Formulation

The main basics of XFEM are briefly recalled in this section, before its application on the fracturing process of anisotropic solids as OPA. Based on a classical Galerkin method, in addition to the usual global shape functions applied to describe generic nodes, some enrichment functions

Materials Research Proceedings **26** (2023) 29-34 https://doi.org/10.21741/9781644902431-5

are added for cracked elements to account for discontinuities in the displacement field, as singularities at the crack-tip. Starting from the general shape functions for the entire domain of nodes, the enriched approximation for the displacement function is defined as [8-12]

$$u^h(x) = \sum_{i \in I} u_i N_i + \sum_{j \in J} b_j N_j H(x) + \sum_{k \in K} N_k \left[ \sum_{l=1}^{4} c_k^l F_l(x) \right] \tag{1}$$

in which $x$ stands for the global coordinate, $N_i$ are the shape functions referred to an arbitrary node $i$, $u_i$ are the corresponding degrees of freedom, $H(x)$ is the Heaviside function which accounts for the displacement jump, $N_j$ refers to the shape function at the discontinuity node $j$, and $b_j$ represents the additional degrees of freedom associated with $H(x)$. Moreover, $F_l(x)$ are the enrichment functions at the crack-tip, $N_k$ are the shape functions associated to the crack-tip functions at node $k$, while $c_k^l$ are the other degrees of freedom for the elastic asymptotic crack-tip enrichment functions.

In an enriched element, the degradation process starts taking place, when some fixed crack initiation criteria are satisfied, which can be referred either to the stress and strain field. In this perspective, we select a maximum nominal stress criterion, i.e.

$$\max \left\{ \frac{\langle p_n \rangle}{p_n^o}, \frac{p_s}{p_s^o}, \frac{p_t}{p_t^o} \right\} = 1 \tag{2}$$

where $\langle \ \rangle$ is the Macauley bracket, and $\mathbf{p}$ is the nominal traction stress vector, defined by means of its normal component $p_n$, and shear components $p_s$, $p_t$, whereas $p_n^o$, $p_s^o$, $p_t^o$ are the associated peak values. Based on relation (2), the damage process starts once the maximum nominal stress ratio reaches the unit value. Such stress components follow the material degradation defined by the damage variable $D$, i.e.

$$p_n = \begin{cases} (1-D)P_n & P_n \geq 0 \\ P_n & \text{otherwise} \end{cases} \tag{3}$$

$$p_s = (1-D)P_s \tag{4}$$

$$p_t = (1-D)P_t \tag{5}$$

where $P_n, P_s, P_t$ stand for the normal and shear stress components as predicted by an elastic traction-separation behavior for an undamaged strain field. On the contrary, for a compressive state $P_n < 0$, the material behaves elastically, without any presence of damage. The scalar damage parameter assumes a null value before the damage initiation, and it increases monotonically up to the unit value, during the damage evolution until the complete damage. More specifically, the damage parameter is assumed to follow an exponential evolution of the type

Materials Research Proceedings **26** (2023) 29-34 https://doi.org/10.21741/9781644902431-5

$$D = 1 - \left\{ \frac{\delta_m^0}{\delta_m^{\max}} \right\} \left\{ 1 - \frac{1 - \exp\left( -\alpha \left( \frac{\delta_m^{\max} - \delta_m^0}{\delta_m^f - \delta_m^0} \right) \right)}{1 - \exp(-\alpha)} \right\} \tag{6}$$

where the damage evolution is represented by the dimensionless parameter $\alpha$, while the effective displacement at the damage initiation, the maximum value of the effective displacement reached during the loading steps and the effective displacement at complete failure are, labeled, respectively, as $\delta_m^0, \delta_m^{\max}$ and $\delta_m^f$.

**Numerical Investigation**

We start now the numerical analysis for the OPA-based SCB, implemented in the code as a transversely isotropic material with bedding planes aligned by 45° with respect to the borehole axis, as suggested in Refs. [5-7]. Elastic properties derived from in-situ and laboratory tests are herein assigned to OPA, according to a quasi-brittle and transversely isotropic constitutive law of the type

$$\begin{Bmatrix} \varepsilon_{xx} \\ \varepsilon_{yy} \\ \varepsilon_{zz} \\ \gamma_{xy} \\ \gamma_{xz} \\ \gamma_{yz} \end{Bmatrix} = \begin{Bmatrix} \frac{1}{E_x} & \frac{-\nu_{xy}}{E_x} & \frac{-\nu_{xz}}{E_z} & 0 & 0 & 0 \\ \frac{-\nu_{xy}}{E_x} & \frac{1}{E_x} & \frac{-\nu_{yz}}{E_z} & 0 & 0 & 0 \\ \frac{-\nu_{xz}}{E_z} & \frac{-\nu_{yz}}{E_z} & \frac{1}{E_z} & 0 & 0 & 0 \\ 0 & 0 & 0 & \frac{2(1+\nu_{xy})}{E_x} = \frac{1}{G_{xy}} & 0 & 0 \\ 0 & 0 & 0 & 0 & \frac{1}{G_{xz}} & 0 \\ 0 & 0 & 0 & 0 & 0 & \frac{1}{G_{xz}} \end{Bmatrix} \begin{Bmatrix} \sigma_{xx} \\ \sigma_{yy} \\ \sigma_{zz} \\ \sigma_{xy} \\ \sigma_{xz} \\ \sigma_{yz} \end{Bmatrix} \tag{7}$$

where $E_z = 4$ GPa, $\nu_{xy} = 0.33$, $\nu_{xz} = 0.24$, $G_{xz} = 1.2$ GPa, with $G_{xy} \neq G_{yz} = G_{xz}$ and $\nu_{xz} = \nu_{yz}$ [7]. The specimen has diameter $D = 80$ mm and thickness $S = 6$ mm, and it is subjected to a downward displacement of $0.1$ mm in the mid-side of the top face (Fig. 1). The specimen is discretized with tetrahedral elements of quadratic geometric order (C3D10), as also applied in the extended work by Dimitri et al. [7]. The damage evolution (defined in the same notation as in the Abaqus code) is controlled by a constitutive law with a softening branch of the following type

$$\frac{p_n}{p_n^0} = 1 - \frac{1 - e^{\frac{-x\delta_m}{\delta_m^f}}}{1 - e^{-\alpha}} \tag{8}$$

where $p_n^0$ is the parallel-to-bedding tensile strength of the material, here kept equal to $2$ MPa; $\delta_m$ is the displacement discontinuity, while $\delta_m^f$ is its associated critical value, assumed as $\delta_m^f = 0.1$ mm; and $\alpha$ is kept equal to 5.

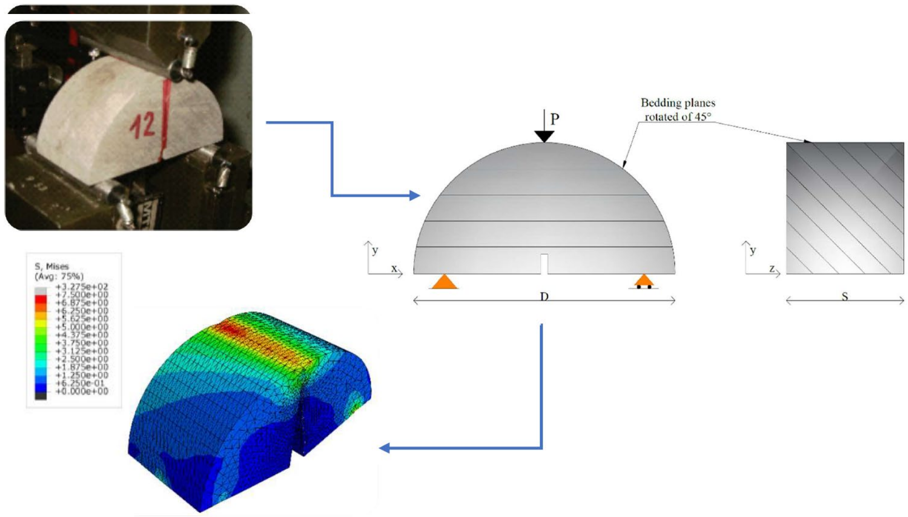


***Figure 1.*** *An SCB test modeled starting from experimental results.*

Based on these assumptions, a sensitivity study is performed to investigate the influence of the notch shape and dimension on the response of the SCB specimen. To this end, four different notch shapes are taken into account as shown in Fig. 2.

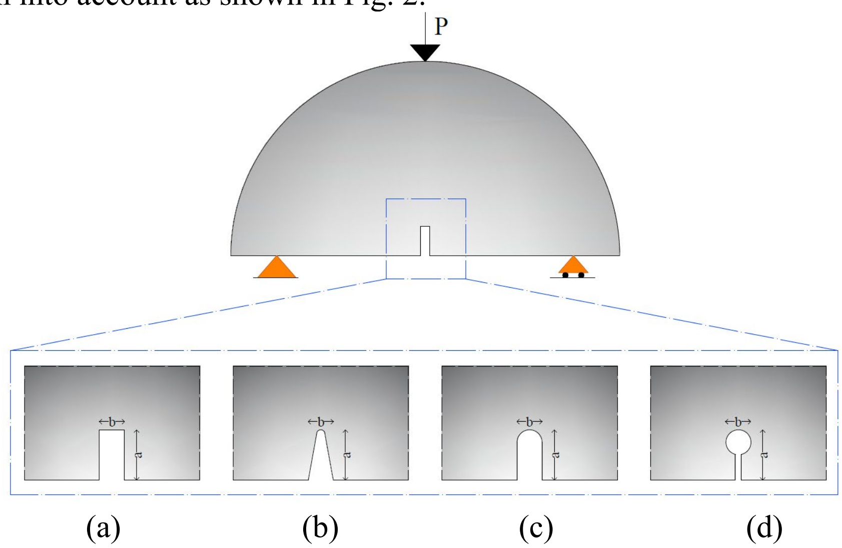


***Figure 2.*** *Notch shapes investigated: (a) rectangular notch, (b) V-notch, (c) U-notch, (d) key-hole like notch.*

The notch depth $a = 6$ mm is kept constant, while the notch width $b$ is varied from 1 mm up to 4 mm by steps of 1 mm. The V-notch tip has a connecting radius of 0.5 mm for each value of $b$, so that, for $b = 1$ mm it reverts to the U-notch with the same dimensions. The global force-CMOD response of the specimens (Fig. 3) shows a slight dependence of the curves to the notch shape at least in the maximum strength and descending branches, with possible variations in the overall ductility, together with small variations in the crack path, around the vertical direction. For each selected notch shape with $b = 2$ mm, in Fig. 4 we display some principal stress contour plots at the same time step.

https://doi.org/10.21741/9781644902431-5

**XFEM**

Notch depth $a = 6\,\text{mm}$

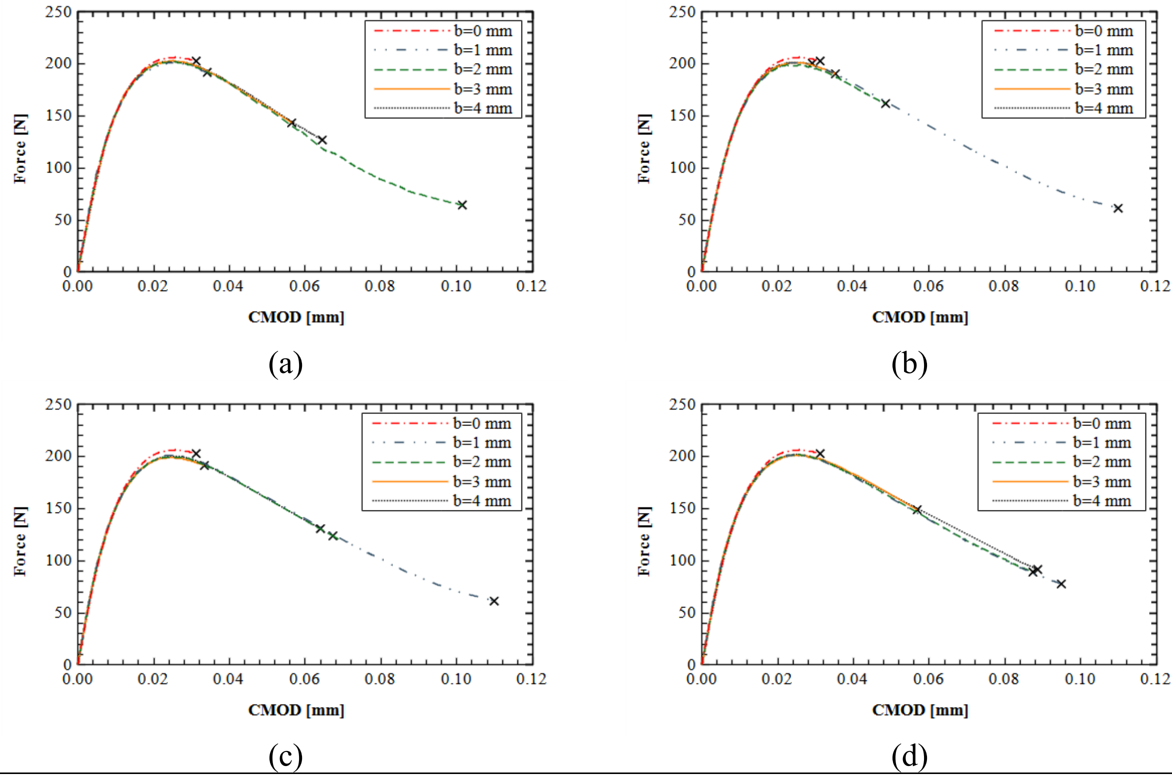


***Figure 3.*** *Force-CMOD response of specimens with* $b$ *varying from 0 mm to 4 mm and with: (a) rectangular notch, (b) U-notch, (c) V-notch, (d) key-hole-like notch.*

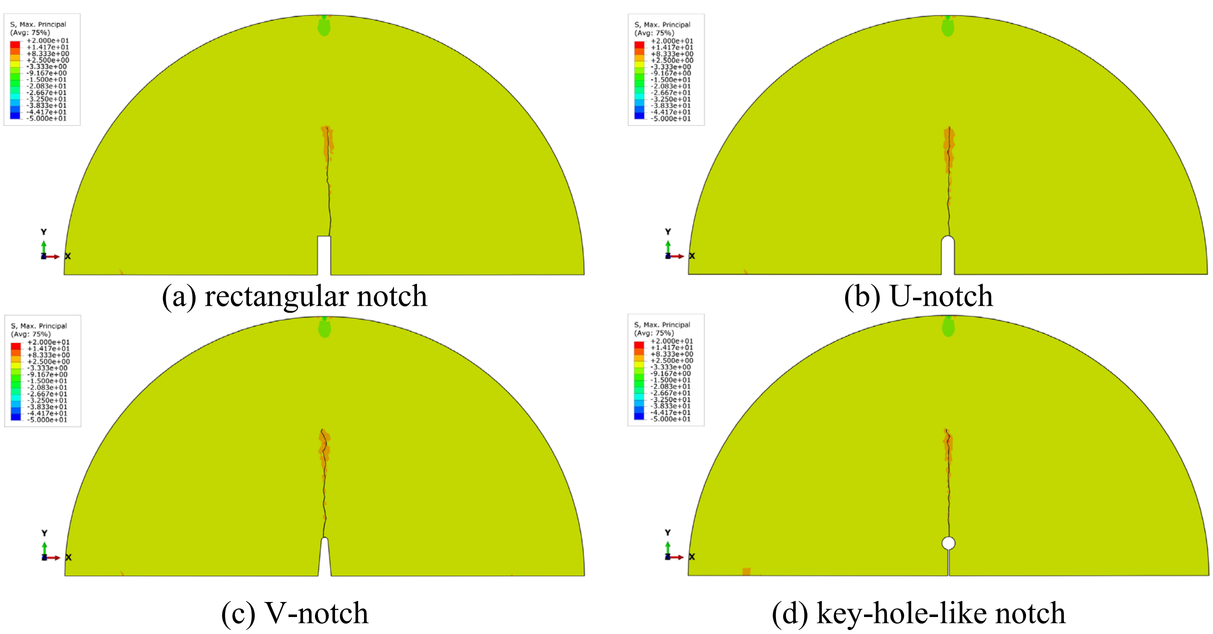


***Figure 4.*** *Principal stress distributions for the specimen with* $a = 6\text{mm}$ *and* $b = 2\text{mm}$.

It is worth observing that the crack propagates in the same vertical direction in all specimens. Furthermore, the principal stress distributions in the entire solid are almost the same for an equal crack length. In addition, the position of the crack initiation corresponds to the notch vertex for the rectangular shape (Fig. 4a), while it is always located in the center of the circular notch tip for the other shapes (Fig. 4b-c-d).

## Conclusion

In the present work, the XFEM-based approach is implemented together with damage mechanics to study the fracturing response of an OPA-based rock, with a transversely isotropic behavior. In line with an experimental investigation from literature [6], a notched Semi-Circular Bending test is explored to assess the influence of the notch shape and size on the overall fracturing response. Based on results, a negligible variation is observed in the ascending branch of the load-CMOD curves, with a more pronounced variation in the peak load and brittleness of the specimen. Such variations come with few deviations of the crack from the vertical direction. A further extension of the work will include the arbitrariness of the bedding properties or the influence of the notch inclination with respect to the bedding planes.

## References

[1] R. McLamore, K.E. Gray, The mechanical behavior of Anisotropic Sedimentary Rocks, Am. Soc. Mechannical Eng. J. Eng. Ind. 89 (1967) 73–6. https://doi.org/10.1115/1.3610013

[2] H. Niandou, J. F. Shao, J. P. Henry, D. Fourmaintraux, Laboratory investigation of the mechanical behaviour of tournemire shale, Int. J. Rock Mech. Min. Sci. 34 (1997) 3–16. https://doi.org/10.1016/S1365-1609(97)80029-9

[3] M. Naumann, U. Hunsche, O. Schulze, Experimental investigations on anisotropy in dilatancy, failure and creep of Opalinus Clay, Phys. Chem. Earth. 32 (2007) 889–895. https://doi.org/10.1016/j.pce.2005.04.006

[4] F. Barpi, S. Valente, M. Cravero, G. Iabichino, C. Fidelibus, Fracture mechanics characterization of an anisotropic geomaterial, Eng. Fract. Mech. 84 (2012) 111–122. https://doi.org/10.1016/j.engfracmech.2012.01.010

[5] H. Bock, P. Blümling, RA Experiment Rock mechancis analysis and synthesis: data report on rock mechanics. TR 2000-02, Mont Terri Technical Report 2000-02. 52 (2001).

[6] S. Valente, C. Fidelibus, S. Loew, M. Cravero, G. Iabichino, F. Barpi, Analysis of fracture mechanics tests on opalinus clay, Rock Mech. Rock Eng. 45 (2012) 767–779. https://doi.org/10.1007/s00603-012-0225-2

[7] R. Dimitri, M. Rinaldi, M. Trullo, F. Tornabene, C. Fidelibus, FEM/XFEM modeling of the 3D fracturing process in transversely isotropic geomaterials, Compos. Struct. 276 (2021) 114502. https://doi.org/10.1016/j.compstruct.2021.114502

[8] T. Belytschko, T. Black, Elastic crack growth in finite elements with minimal remeshing, Int. J. Numer. Methods Eng. 45 (1999) 601–620. https://doi.org/10.1002/(SICI)1097-0207(19990620)45:5<601::AID-NME598>3.0.CO;2-S

[10] N. Moës, J. Dolbow, T. Belytschko, A finite element method for crack growth without remeshing, Int. J. Numer. Methods Eng. 46 (1999) 131–150. https://doi.org/10.1002/(SICI)1097-0207(19990910)46:1<131::AID-NME726>3.0.CO;2-J

[11] J. Dolbow, An extended finite element method with discontinuous enrichment for applied mechanics, (2000).

[12] J. Dolbow, N. Moës, T. Belytschko, Discontinuous enrichment in finite elements with a partition of unity method, Finite Elem. Anal. Des. 36 (2000) 235–260. https://doi.org/10.1016/S0168-874X(00)00035-4